

Robust Feature Tracking in Underwater Video Sequences

T. Tommasini, A. Fusiello, V. Roberto

Machine Vision Laboratory
Dipartimento di Matematica e Informatica
Università di Udine, IT

{tommasin,fusiello,roberto}@dimi.uniud.it

E. Trucco

Computer Vision Group and Ocean Systems Laboratory
Department of Computing and Electrical Engineering
Heriot-Watt University, UK

mtc@cee.hw.ac.uk

Abstract— This paper proposes a robust feature tracker based on an efficient outlier rejection scheme, suitable for feature tracking in subsea video sequences. We extend the Shi-Tomasi-Kanade scheme by introducing a technique for rejecting spurious features. We employ a simple and efficient outlier rejection rule, called X84, and prove that its theoretical assumptions are satisfied in the feature tracking scenario. Experiments with synthetic and real subsea sequence confirm that our algorithm locates and discards unreliable features accurately and consistently, and tracks good features reliably over many frames. We also illustrate quantitatively the benefits introduced by the algorithm with the example of fundamental matrix estimation.

I. Introduction

Feature tracking is an important issue in computer vision, as many algorithms rely on the accurate computation of correspondences through a sequence of images [1], [2], [3]. Two important examples are depth ranging by stereo and visual servoing (e.g., estimation of vehicle motion relative to a target, station keeping, hovering).

When an image sequence is acquired and sampled at a sufficiently high time frequency, frame-to-frame disparities are small enough to make optical-flow techniques viable [4]. If frame-to-frame disparities are large (e.g., the images are taken from quite different viewpoints), stereo matching techniques [5] are used instead, often in combination with Kalman filtering [6], [7], [8]. *Robust tracking* means detecting automatically unreliable matches, or *outliers*, over an image sequence (see [9] for a survey of robust methods in computer vision). Recent examples of such robust algorithms include [10], which identifies tracking outliers while estimating the fundamental matrix, and [11], which adopts a RANSAC approach to eliminate outliers for estimating the trifocal tensor. Such approaches increase the computational cost of tracking significantly.

This paper concentrates on the well-known Shi-Tomasi-Kanade tracker, and proposes a robust version based on an efficient outlier rejection scheme. Building

on results from [12], Tomasi and Kanade [13] introduced a feature tracker based on SSD matching and assuming translational frame-to-frame displacements. Subsequently, Shi and Tomasi [14] proposed an *affine model*, which proved adequate for region matching over longer time spans. Their system classified a tracked feature as *good* (reliable) or *bad* (unreliable) according to the residual of the match between the associated image region in the first and current frames; if the residual exceeded a user-defined threshold, the feature was rejected. Visual inspection of results demonstrated good discrimination between good and bad features, but the authors did not specify how to reject bad features *automatically*.

This is the problem that our paper solves. We extend the Shi-Tomasi-Kanade tracker (Section 2) by introducing an *automatic* scheme for rejecting spurious features. We employ a simple, efficient, model-free outlier rejection rule, called X84, and prove that its assumptions are satisfied in the feature tracking scenario (Section 3). Experiments with synthetic and real subsea sequences confirming that our algorithm locates and discards unreliable features accurately and consistently, and tracks good features reliably over many frames (Section 4). We illustrate quantitatively the benefits introduced by the algorithm with the example of fundamental matrix estimation. The complete code of the robust tracker is available via ftp at: <ftp://taras.dimi.uniud.it/pub/sources/rtrack.tar.gz>.

II. The Shi-Tomasi-Kanade tracker

In this section the Shi-Tomasi-Kanade tracker [14], [13] will be briefly described. Consider an image sequence $I(\mathbf{x}, t)$, with $\mathbf{x} = [u, v]^T$, the coordinates of an image point. If the time sampling frequency is sufficiently high, we can assume that small image regions are displaced but their intensities remain unchanged:

$$I(\mathbf{x}, t) = I(\delta(\mathbf{x}), t + \tau), \quad (1)$$

where $\delta(\cdot)$ is the *motion field*, specifying the *warping* that is applied to image points. The fast-sampling hypothesis allows us to approximate the motion with a translation, that is, $\delta(\mathbf{x}) = \mathbf{x} + \mathbf{d}$, where \mathbf{d} is a displacement vector. The tracker's task is to compute \mathbf{d} for a number of selected points for each pair of successive frames in the sequence.

As the image motion model is not perfect, and because of image noise, Eq. (1) is not satisfied exactly. The problem is then finding the displacement $\hat{\mathbf{d}}$ which minimizes the SSD residual:

$$\epsilon = \sum_{\mathcal{W}} [I(\mathbf{x} + \mathbf{d}, t + \tau) - I(\mathbf{x}, t)]^2 \quad (2)$$

where \mathcal{W} is a small image window centered on the point for which \mathbf{d} is computed. By plugging the first-order Taylor expansion of $I(\mathbf{x} + \mathbf{d}, t + \tau)$ into (2), and imposing that the derivatives with respect to \mathbf{d} are zero, we obtain the linear system

$$G\mathbf{d} = \mathbf{e}, \quad (3)$$

where

$$G = \sum_{\mathcal{W}} \begin{bmatrix} I_u^2 & I_u I_v \\ I_u I_v & I_v^2 \end{bmatrix}, \quad \mathbf{e} = -\tau \sum_{\mathcal{W}} I_t [I_u \ I_v]^\top,$$

with $[I_u \ I_v] = \nabla I = [\partial I / \partial u \ \partial I / \partial v]$ and $I_t = \partial I / \partial t$. The tracker is based on Eq. (3): given a pair of successive frames, the solution of (3), that is, $\hat{\mathbf{d}} = G^{-1}\mathbf{e}$, is used to predict a new (registered) frame. The procedure is iterated according to a Newton-Raphson scheme, until convergence of the displacement estimates.

A. Feature extraction

In this framework, a feature can be tracked reliably if a numerically stable solution to Eq. (3) can be found, which requires that G is well-conditioned and its entries are well above the noise level. In practice, since the larger eigenvalue is bounded by the maximum allowable pixel value, the requirement is that the smaller eigenvalue is sufficiently large. Calling λ_1 and λ_2 the eigenvalues of G , we accept the corresponding feature if $\min(\lambda_1, \lambda_2) > \lambda$, where λ is a user-defined threshold [14].

B. Affine Model

The translational model cannot account for certain transformations of the feature window, for instance rotation, scaling, and shear. An *affine motion field* is a more accurate model [14], that is,

$$\delta(\mathbf{x}) = A\mathbf{x} + \mathbf{d}, \quad (4)$$

where \mathbf{d} is the displacement, and A is a 2×2 matrix accounting for affine warping, and can be written as $A = \mathbf{1} + D$, with $D = [d_{ij}]$ a deformation matrix and $\mathbf{1}$ the identity matrix. Similarly to the translational case,

one estimates the motion parameters, D and \mathbf{d} , by minimizing the residual

$$\epsilon = \sum_{\mathcal{W}} [I(A\mathbf{x} + \mathbf{d}, t + \tau) - I(\mathbf{x}, t)]^2. \quad (5)$$

By plugging the first-order Taylor expansion of $I(A\mathbf{x} + \mathbf{d}, t + \tau)$ into (5), and imposing that the derivatives with respect to D and \mathbf{d} are zero, we obtain the linear system

$$T\mathbf{z} = \mathbf{a}, \quad (6)$$

in which $\mathbf{z} = [d_{11} \ d_{12} \ d_{21} \ d_{22} \ d_1 \ d_2]^\top$ contains the unknown motion parameters, and

$$\mathbf{a} = -\tau \sum_{\mathcal{W}} I_t [u I_u \ u I_v \ v I_u \ v I_v \ I_u \ I_v]^\top,$$

$$T = \sum_{\mathcal{W}} \begin{bmatrix} U & V \\ V^\top & G \end{bmatrix},$$

with

$$U = \begin{bmatrix} u^2 I_u^2 & u^2 I_u I_v & uv I_u^2 & uv I_u I_v \\ u^2 I_u I_v & u^2 I_v^2 & uv I_u I_v & uv I_v^2 \\ uv I_u^2 & uv I_u I_v & v^2 I_u^2 & v^2 I_u I_v \\ uv I_u I_v & uv I_v^2 & v^2 I_u I_v & v^2 I_v^2 \end{bmatrix},$$

$$V^\top = \begin{bmatrix} u I_u^2 & u I_u I_v & v I_u^2 & v I_u I_v \\ u I_u I_v & u I_v^2 & v I_u I_v & v I_v^2 \end{bmatrix}.$$

Again, Eq. (6) is solved for \mathbf{z} using a Newton-Raphson iterative scheme. If frame-to-frame affine deformations are negligible, the pure translation model is preferable (the matrix A is assumed to be the identity).

III. Robust Monitoring

To monitor the quality of the features, the tracker checks the residuals between the first and the current frame: high residuals indicate bad features which must be rejected. Following [14], we adopt the affine model, as a pure translational model would not work well with long sequences: too many good features are likely to undergo significant rotation, scaling or shearing, and would be incorrectly discarded. Non-affine warping, which will yield high residuals, is caused by occlusions, perspective distortions and strong intensity changes (e.g. specular reflections). This section introduces our method for selecting a robust rejection threshold *automatically*.

A. Distribution of the residuals

We begin by establishing which distribution is to be expected for the residuals when comparing good features, i.e, almost identical regions. We assume that the intensity $I(\delta(\mathbf{x}), t)$ of each pixel in the current-frame region is equal to the intensity of the corresponding pixel in the first frame $I(\mathbf{x}, 0)$ plus some Gaussian noise $n \simeq \eta(0, 1)$. Hence

$$I(\delta(\mathbf{x}), t) - I(\mathbf{x}, 0) \simeq \eta(0, 1).$$

Since the square of a Gaussian random variable has a chi-square distribution, we obtain

$$[I(\delta(\mathbf{x}), t) - I(\mathbf{x}, 0)]^2 \simeq \chi^2(1).$$

The sum of n chi-square random variables with one degree of freedom is distributed as a chi-square with n degrees of freedom (as it is easy to see by considering the moment-generating functions). Therefore, the residual computed according to (2) over a $N \times N$ window \mathcal{W} is distributed as a chi-square with N^2 degrees of freedom:

$$\epsilon = \sum_{\mathcal{W}} [I(\delta(\mathbf{x}), t) - I(\mathbf{x}, 0)]^2 \simeq \chi^2(N^2). \quad (7)$$

As the number of degrees of freedom increases, the chi-square distribution approximates a Gaussian, which is in fact used to approximate the chi-square whenever $N > 30$. Therefore, since the window \mathcal{W} associated to each feature is at least 7×7 , we can safely assume a Gaussian distribution of the residual for the good features:

$$\epsilon \simeq \eta(N^2, 2N^2).$$

B. The X84 rejection rule

When the two regions over which we compute the residual are bad features (they are not warped by an affine transformation), the residual is not a sample from the normal distribution of good features: it is an outlier. Hence, the detection of bad features reduces to a problem of outlier detection, which is equivalent to the problem of estimating the mean and variance of the corrupted Gaussian distribution. To do this, we employ a simple but effective model-free rejection rule, X84 [15], which achieves robustness by employing median and median deviation instead of the usual mean and standard deviation. This rule prescribes to reject values which are more than k Median Absolute Deviations (MADs) away from the median:

$$\text{MAD} = \text{med}_i \{ |\epsilon_i - \text{med}_j \epsilon_j| \}. \quad (8)$$

In our case, ϵ_i are the tracking residuals. A value of $k = 5.2$, is adequate in practice, as it corresponds to about 3.5 standard deviations, and the range $[\mu - 3.5\sigma, \mu + 3.5\sigma]$ contains more than the 99.9% of a Gaussian distribution [15]. The rejection rule X84 has a breakdown point of 50%: any majority of the data can overrule any minority.

C. Photometric normalisation

Our robust implementation of the Shi-Tomasi-Kanade tracker incorporates also a *normalised* SSD matcher for residual computation. This limits the effects of intensity changes between frames, by subtracting the average grey level (μ_J, μ_I) and dividing by the standard deviation (σ_J, σ_I) in each of the two regions considered:

$$\epsilon = \sum_{\mathcal{W}} \left[\frac{J(A\mathbf{x} + \mathbf{d}) - \mu_J}{\sigma_J} - \frac{I(\mathbf{x}) - \mu_I}{\sigma_I} \right]^2. \quad (9)$$

where $J(\cdot) = I(\cdot, t + 1)$, $I(\cdot) = I(\cdot, t)$.

A more elaborate normalisation is described in [16]; [17] reports a modification of the Shi-Tomasi-Kanade tracker based on explicit photometric models.

IV. Experimental results

We evaluated our tracker in a series of experiments, of which we report three. The *Platform* sequence is a 20-frame synthetic sequence of 256×256 images, generated on a Silicon Graphics Indy. It simulates a vehicle moving around an imaginary platform sitting on a sandy floor, which is a grey-level rendering of a sonar sidescan. The sequence is part of the SOFA (Sequences for Optical Flow Analysis) public-domain set of test sequences available at <http://www.cee.hw.ac.uk/~mtc/sofa>. The *Hyball* sequence was acquired by a Hydrovision Hyball ROV in the test tank of the Ocean Systems Laboratory at Heriot-Watt University. It consists of 31 grey-level frames, each of 170×256 pixel. The *Smallrock* sequence of 170×256 frames was acquired by a ROV on a scientific mission in the Mediterranean sea. Figures 1, 3 and 5 show, for each sequence, the first frame with extracted features superimposed and the last frame with features and trajectories superimposed. Filled windows indicate features rejected by the robust tracker. MPEG sequences are available on the Internet from <http://www.dimi.uniud.it/~fusiello/>.

In Figures 2, 4 and 6 the residuals of all features against the frame number are plotted. The horizontal line indicate the threshold set automatically by X84.

The effect of aliasing in the *Platform* sequence, which is synthetic, is clearly visible. The rejected features number 23, 28, 32 slightly shifted during the tracking, hence they are correctly rejected. Features number 5, 21, 26 are attached to the correct point, but they undergo a strong deformation.

In the *Hyball* sequence, features 30 and 32 end up superimposed. Features 21 is rejected because of the marked shape deformation, whereas feature 26 undergoes a severe brightness change.

In the *Smallrock* sequence, all features are good, but the ones with the higher residual are rejected anyway. Yet, false negatives like in this case are not as dangerous as false positives (fail to reject an outlier), which never occurred in our experiments.

To illustrate quantitatively the benefits of our robust tracker, we used the tracked features to compute the fundamental matrix between the first and last frame of the three sequences. We used the nonlinear method based on distances between points and epipolar lines, implemented by Zhang [3]. As a measure of the goodness of the estimated epipolar geometry, we took the RMS distance of the tracked points from the corresponding epipolar lines: if the epipolar geometry is estimated exactly, all points should lie on epipolar lines. The results are shown in Table 1. In one case we used all the features, in the other we discarded some of them, according to the X84 rejection rule. With all the sequences, the robust tracker brings a decrease in the RMS distance.

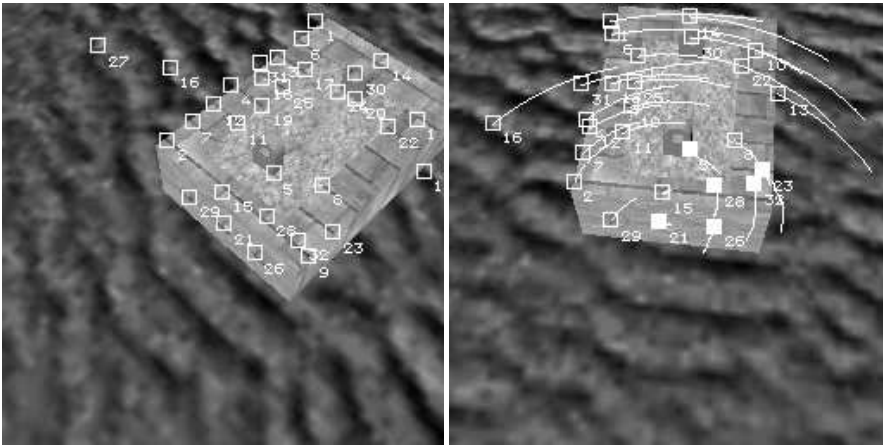


Fig. 1: First and last frame of the *Platform* sequence. The filled windows in the last frames indicate features rejected by X84.

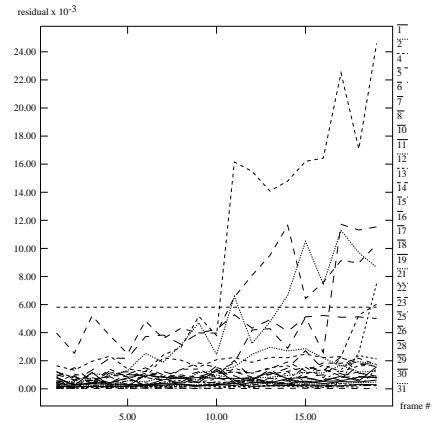


Fig. 2: Residuals magnitude against frame number for *Platform*. The arrows indicate the threshold set by X84.

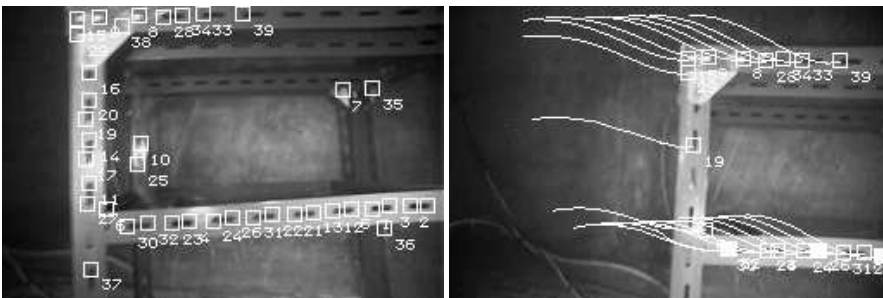


Fig. 3: First and last frame of the *Hyball* sequence.

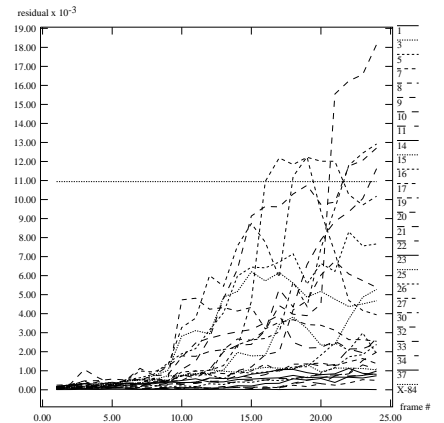


Fig. 4: Residuals magnitude against frame number for *Hyball*.



Fig. 5: First and last frame of the *Smallrock* sequence. The filled windows in the last frames indicate features rejected by X84.

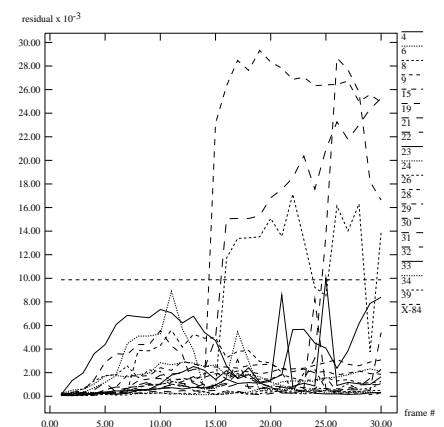


Fig. 6: Residuals magnitude against frame number for *Smallrock*.

Table 1: RMS distance of points from epipolar lines.

	Platform	Hyball	Smallrock
All	1.88	0.23	0.58
X84	1.63	0.18	0.53

V. Conclusions

We have presented a robust extension of the Shi-Tomasi-Kanade tracker, based on the X84 outlier rejection rule. The computational cost is much less than that of schemes based on robust regression and random sampling like RANSAC or LMedSq [9], [11], yet experiments indicate excellent reliability in the presence of non-affine feature warping (most reliable features preserved, all unreliable features rejected). Our experiments have also pointed out the pronounced sensitivity of the Shi-Tomasi-Kanade tracker to illumination changes. We believe that our robust tracker can be useful to the large community of researchers needing efficient and reliable trackers. To facilitate dissemination and enable direct comparisons and experimentation, we have made the code available on the Internet.

Acknowledgements

This work was supported by a British Council-MURST/CRUI grant, and by the EU programmes SOCRATES and MAST (contract MAS3-CT97-0083 "ARAMIS", Advanced ROV Package for Automatic Investigation of Sediments). Thanks to Chris Smith of the Institute of Marine Biology of Crete for the *Smallrock* data, and to Stuart Clarke of the Heriot-Watt Image Analysis Laboratory for the sidescan seabed image used in *Platform*.

References

- [1] L. Robert, C. Zeller, O. Faugeras, and M. Hébert, "Applications of non-metric vision to some visually-guided robotics tasks," in *Visual Navigation: From Biological Systems to Unmanned Ground Vehicles*, Y. Aloimonos, Ed., chapter 5, pp. 89–134. Lawrence Erlbaum Associates, 1997.
- [2] C. Tomasi and T. Kanade, "Shape and motion from image streams under orthography – a factorization method," *International Journal of Computer Vision*, vol. 9, no. 2, pp. 137–154, November 1992.
- [3] Z. Zhang, "Determining the epipolar geometry and its uncertainty: A review," Tech. Rep. 2927, INRIA Sophia-Antipolis, France, July 1996.
- [4] J. L. Barron, D. J. Fleet, and S. Beauchemin, "Performance of optical flow techniques," *International Journal of Computer Vision*, vol. 12, no. 1, pp. 43–77, 1994.
- [5] A. Fusiello, V. Roberto, and E. Trucco, "Efficient stereo with multiple windowing," in *Proceedings of the IEEE Conference on Computer Vision and Pattern Recognition*, Puerto Rico, June 1997, pp. 858–863, IEEE Computer Society Press.
- [6] L. Matthies, T. Kanade, and R. Szelisky, "Kalman filter based algorithms for estimating depth from image sequences," *International Journal of Computer Vision*, vol. 3, pp. 209–236, 1989.
- [7] L.S. Shapiro, H. Wang, and J.M. Brady, "A matching and tracking strategy for independently moving objects," in *Proceedings of the British Machine Vision Conference*. BMVA Press, 1992, pp. 306–315.
- [8] E. Trucco, V. Roberto, S. Tinonin, and M. Corbato, "SSD disparity estimation for dynamic stereo," in *Proceedings of the British Machine Vision Conference*, R. B. Fisher and E. Trucco, Eds. BMVA Press, 1996, pp. 342–352.
- [9] P. Meer, D. Mintz, D. Y. Kim, and A. Rosenfeld, "Robust regression methods in computer vision: a review," *International Journal of Computer Vision*, vol. 6, pp. 59–70, 1991.
- [10] P. H. S. Torr, A. Zisserman, and S. Maybank, "Robust detection of degeneracy," in *Proceedings of the IEEE International Conference on Computer Vision*, E. Grimson, Ed. 1995, pp. 1037–1044, Springer-Verlag.
- [11] P. H. S. Torr and A. Zisserman, "Robust parameterization and computation of the trifocal tensor," in *British Machine Vision Conference*, R. Fisher and E. Trucco, Eds. September 1996, pp. 655–664, BMVA, Edinburgh.
- [12] B. D. Lucas and T. Kanade, "An iterative image registration technique with an application to stereo vision," in *Proceedings of International Joint Conference on Artificial Intelligence*, 1981.
- [13] C. Tomasi and T. Kanade, "Detection and tracking of point features," Technical Report CMU-CS-91-132, Carnegie Mellon University, Pittsburg, PA, April 1991.
- [14] J. Shi and C. Tomasi, "Good features to track," in *Proceedings of the IEEE Conference on Computer Vision and Pattern Recognition*, June 1994, pp. 593–600.
- [15] F.R. Hampel, P.J. Rousseeuw, E.M. Ronchetti, and W.A. Stahel, *Robust Statistics: the Approach Based on Influence Functions*, Wiley Series in probability and mathematical statistics. John Wiley & Sons, 1986.
- [16] I.J. Cox, S. Roy, and S.L. Hingorani, "Dynamic histogram warping of image pairs for constant image brightness," in *Proceedings of the IEEE International Conference on Image Processing*, 1995, pp. 366–369.
- [17] G.D. Hager and P.N. Belhumeur, "Real-time tracking of image regions with changes in geometry and illumination," in *Proceedings of the IEEE Conference on Computer Vision and Pattern Recognition*, 1996, pp. 403–410.